

99-203

Environment Canada

Water Science and Technology Directorate

Direction générale des sciences
et de la technologie, eau

Environnement Canada

Investigation of Radial Diffusion in Dolostone Core
Samples from the Lockport Formation, Smythville,

Ontario: Phase II

By:

L. Zanini, K. Novakowski, G. Bickerton

TD
226
N87
No. 99-
203

99-203

**Investigation of Radial Diffusion in Dolostone Core Samples from the Lockport
Formation, Smithville, Ontario: Phase II**

by:

Lavinia Zanini, Kent Novakowski and Greg Bickerton

Groundwater Assessment and Restoration Project
National Water Research Institute
Environment Canada
867 Lakeshore Rd
Burlington, Ontario, Canada

NWRI Contribution No. 99 - 203
January, 1999

Abstract

Dolostone samples from the geological units which comprise the Lockport Formation, were collected from core samples obtained from boreholes drilled near Smithville, Ontario. These samples were used in forward and reverse diffusion tracer experiment to estimate the effective porosity of the dolostone units and determine the effective diffusion coefficients, and thus a geometric factor, for specific chemical tracers. The experiments were conducted using radial diffusion cells of various dimensions.

Several samples were collected from each of the geological units of the Lockport Formation and from the underlying Rochester Formation. Radial diffusion cells were constructed and experiments were initiated by monitoring tracer concentrations as they diffused into the rock matrix. The tracers used included bromide (as KBr), Lissamine FF (a conservative organic dye), nitrite (as NaNO_2) and Difluorobenzoic acid (DFBA).

Current analytical procedures and experimental methods for the radial diffusion method were found to predict the total gravimetric porosity within a range of 1 to 2%. Although this error may be considered minor in some studies, it is too large to distinguish an effective porosity. Analytical procedures also lack adequate sensitivity to determine precise effective diffusion coefficients. Errors in the effective diffusion coefficient are propagated in the calculation of the geometric factor. The study has determined that Lissamine FF does not behave conservatively during forward diffusion experiments. However, DFBA was found to be a conservative tracer in all experiments. Future investigations should explore the use of DFBA as a field tracer at the Smithville site.

Table of Contents

Abstract.....	i
List of Tables.....	iii
List of Figures.....	iv
Introduction.....	1
Methods.....	1
Results and Discussion.....	4
Tracer behavior.....	4
Effective porosity.....	5
Effective diffusion coefficient.....	6
Conclusions.....	8
References.....	9
Acknowledgments.....	9
Appendix A.....	30

List of Tables

Table 1: Cell locations and dimensions.....	10
Table 2: Physical description of samples used for diffusion cells.....	11
Table 3: Measured reservoir volume for each test (mL).....	13
Table 4: Tracer type used during radial diffusion experiments.....	14
Table 5: Model predicted effective porosity (Retardation = 1) and gravimetric porosity results in %.....	15
Table 6: Calculated porosity from steady-state concentrations using $B = V_r/\theta_e\gamma_{rR}$; corrected for mass loss due to sampling.....	16
Table 7: Calculated porosity from steady-state concentrations using $B = V_r/\theta_e\gamma_{rR}$; not corrected for mass loss due to sampling.....	17
Table 8: Model predicted effective diffusion coefficients.....	18
Table 9: Calculated geometric factors.....	19
Table A1: Experimental data for forward radial diffusion experiments: Lissamine.....	31
Table A2: Experimental data for forward radial diffusion experiments: Bromide.....	32
Table A3: Experimental data for reverse radial diffusion experiments: Lissamine.....	34
Table A4: Experimental data for reverse radial diffusion experiments: Bromide	35
Table A5: Experimental data for forward radial diffusion experiments: Nitrite	36
Table A6: Experimental data for forward radial diffusion experiments: DFBA	37

List of Figures

Figure 1: Diagram of a radial diffusion cell.....	20
Figure 2a: Forward diffusion experimental and simulated concentration curves: Lissamine and Bromide.....	21
Figure 2b: Forward diffusion experimental and simulated concentration curves: Bromide and DFBA.....	24
Figure 2c: Forward diffusion experimental and simulated concentration curves: Nitrite.....	27
Figure 2d: Reverse diffusion experimental and simulated concentration curves: Lissamine and Bromide.....	28

Introduction

During the late 1970's and early 1980's a PCB waste management site was operating on the outskirts of the town of Smithville, located approximately 15 km south of Lake Ontario, on the Niagara escarpment. In 1985, it was discovered that PCB oils and associated solvents had penetrated the into the ground and pervaded the upper horizons of the bedrock underlying the site. This resulted in the closure of a local water supply which utilized groundwater from this aquifer.

Dolostone samples representing the geological units, which comprise the Lockport Formation, were collected from core samples obtained from boreholes drilled in the vicinity of Smithville, Ontario. These samples were used in forward and reverse diffusion experiments conducted in the laboratory using radial diffusion cells of various dimensions (Novakowski and van der Kamp, 1996; van der Kamp et al., 1996). The purpose of the experiments was to estimate the effective porosity of the dolostone units and determine the effective diffusion coefficients for specific chemical tracers. From the estimates of the effective diffusion coefficient, a geometric factor, which represents the geometry of the pore structure, was also determined (Novakowski and van der Kamp, 1996).

Measurements of the geometric factor allow for the estimation of effective diffusion coefficients for other solutes, such as the organic contaminants which are present in the groundwater near the old PCB contaminated site. This information is required for the accurate prediction of mass transfer from contaminants transported in fractures in the dolostone to the adjacent rock matrix. Small errors in the estimate of the effective diffusion coefficient, and therefore geometric factor, can lead to significant errors in the estimates of mass transferred to the matrix. Thus, the parameters determined in the diffusion study are necessary for the correct interpretation of field tracer experiments, which are used to directly measure the transfer process, and for use in numerical models that are used to simulate this transfer.

Methods

Each of the samples used for this study was collected and preserved in the field at the time of drilling. In all cases, samples were maintained under saturated conditions in

order to avoid the difficulties encountered in re-saturating low-porosity samples (Langer, 1997). The cores are 45 mm in diameter and range from 10 to 20 cm in length (Table 1).

Several samples were collected from each geological unit of the Lockport Formation and from the underlying Rochester Formation (Table 1). The location, dimension and physical description were recorded for each sample (Tables 1 and 2). Radial diffusion cells were constructed by drilling a 1.25 mm diameter reservoir through the center of the core samples, parallel to the core axis (Figure 1). The drilling was conducted using a diamond core bit cooled with groundwater obtained from the site. Each end of the sample was planed to 90° and then the entire sample was encapsulated in a Teflon® sleeve and sealed with two stainless steel end caps. One of the end caps contained a sampling port through which samples were extracted from the reservoir. The Teflon® coating was heat sealed to minimize leaking or evaporation of the liquid phase.

To initiate the forward diffusion experiments, groundwater in the reservoir was removed and replaced with groundwater containing tracer concentrations. The exact volume of tracer solution introduced to each reservoir is given in Table 3. The subsequent decrease in tracer concentration in the reservoir was monitored by periodic sampling (Experimental results given in Appendix A). The sampling was conducted so as to minimize the volume of sample abstracted and at a frequency that well-defines the decline in concentration. It was assumed that free water diffusion maintained uniform concentrations in the reservoir. For comparative purposes, a control cell was constructed using a stainless steel blank of dimensions similar to the rock core.

The tracers used (Table 4) included bromide (as KBr), Lissamine FF (a conservative organic dye), Nitrite (as NaNO₂) and Difluorobenzoic acid (DFBA). Initial concentrations in the reservoir ranged from 500 ppb for Lissamine to 1000 ppm for Bromide (Br), Nitrite (NO₂) and DFBA.

Only tracers assumed to be conservative were chosen so as to eliminate other potential sources of mass loss, such as decay and adsorption. Previous experiments (Shackelford et al., 1989) have shown that Br will behave conservatively in most soils and rock types. Although some organic dyes are known to interact with geological materials (Smart and Laidlaw, 1977), Lissamine was observed to behave conservatively in field-

scale tracer experiments conducted in rock similar to that used for the present experiments (Novakowski and Lapcevic, 1994) and in field experiments conducted at the Smithville site (Novakowski et al., 1999). Difluorobenzoic acid has recently been observed to act conservatively in bench scale studies as well as in aquifer tracer tests (Bowman and Gibbens, 1992).

Following the initiation of the experiment, the reservoir was periodically measured for tracer concentration. A thirty to forty day period was required for the experiments to reach equilibrium (concentration within the reservoir equal to the concentration in the rock). For each Br, NO₂ or DFBA sample obtained, 0.1 to 0.45 mL was abstracted from the reservoir and replaced with deionized water. Lissamine analyses is non-destructive and sample volumes abstracted were immediately returned to the reservoir following analyses. Lissamine was analyzed using a Turner fluorometer. Concentrations of Br⁻ and NO₂ were analyzed, after diluting the sample in distilled water, using a Waters WISP 712 ion chromatograph. In some cases, Br was analyzed with DFBA using high performance liquid chromatography (HPLC) with a variable wavelength UV detector and a strong anion exchange column (Bowman and Gibbens, 1992). Initially, DFBA was analyzed using ion chromatography (for cells, G1, E1, E2, E3 and G3), however this analytical procedure was found to lack adequate sensitivity and later analyses for DFBA were performed using the HPLC.

Once the forward diffusion experiments were completed, reverse diffusion experiments were conducted on some of the cells (Table 4). These experiments were accomplished by replacing the reservoir fluid with deionized water and then monitoring Lissamine and Br tracers as they diffused back into the reservoir in a fashion following that of the forward diffusion experiments. The experiments were conducted to determine if the process of reverse diffusion is the same as that of diffusion from the reservoir into the matrix.

The weight of the cells was monitored over the entire experimental period. Diffusion cells showed an average mass loss of 0.01 mL per day. Mass loss may have occurred from non-visible leaks or evaporation.

To display the results of the diffusion experiments, the concentrations of each tracer (C) were plotted relative to the initial concentrations (C_0) against time. The relative tracer concentrations were modeled using RADIF2 (Novakowski and van der Kamp, 1996) to obtain estimates of the effective diffusion coefficient and effective porosity. RADIF2 is a diffusion model that accounts for radial diffusion, mass balance in the reservoir, linear adsorption, decay and periodic volume extraction of reservoir samples.

For comparison to the modeled results, gravimetric porosity (total porosity) measurements of the rock cores were conducted on all cells after the diffusion experiments were completed. To conduct this measurement, the wet weight of each sample was recorded. Samples were then placed in a drying oven at 50°C for 18 hours and allowed to cool before re-weighing. Porosity was calculated by converting the weight of water lost to a volume and dividing this by the volume of the sample.

Results and Discussion

Tracer behavior

Visual comparison of the relative concentration versus time curves produced by forward diffusion (Figure 2a) indicates that, compared to Br, Lissamine interacted significantly with the rock material. Model-predicted porosity (Table 5) for the forward Lissamine tracer tests are also four times as high than that predicted using Br. Bromide is well known to be conservative in most types of geological materials. Thus, Lissamine does not behave as a conservative tracer during these experiments. The explanation for this behavior, however, is not readily apparent. Adsorption to the matrix material, either by binding to a small quantity of organic matter in the rock or to minute clay particles represents one possibility. For example, stylolites, which are thin, organic-rich beds, are observed in some of the samples at mm scales (Table 2). In addition, previous XRF analyses (Bickerton, 1997) indicate that a small quantity of clay minerals may be present in the rock. It is important to note that Lissamine is not retarded compared to Br in the reverse radial diffusion experiments (Figure 2d) suggesting that much of the initial Lissamine adsorbed is irreversible. In addition, the loss and potential adsorption was not

observed in field-scale experiments, thus the mechanism of mass loss observed during the forward diffusion experiments remains unclear.

However, due to this limitation, Lissamine was not employed any further as a tracer for use in forward radial diffusion experiments. An alternative tracer, DFBA was used instead. Thus, the following discussion is focused primarily on the tracer experiments conducted using Br and DFBA tracers. It was observed that the behavior of NO₂ tracer closely resembled that of Br and thus, for the remainder of the radial diffusion experiments only Br and DFBA tracers were used.

Effective porosity

On average, porosity predicted by reverse diffusion experiments estimated a lower porosity (1 to 2%) using the same tracer, than the forward diffusion experiments (Table 5, Figures 2a and d). Also, reverse diffusion porosities more closely mimicked that of the measured gravimetric porosity.

Forty-five percent of both the forward DFBA and Br tracer experiments (Figure 2b) predicted the exact same porosity and 82% agree within a 2% difference. Forward diffusion experiments using Br and NO₂ overwhelmingly (80%) over-predicted the total gravimetric porosity by an average of 1.6%, and to a lesser extent so did the forward DFBA experiments by an average of 1.7% (Figures 2a, b and c). The reason for this is uncertain. High ion concentrations naturally occurring in the groundwater used in the reservoir may have resulted in analytical interference. However, interference in the analytical procedure was virtually eliminated when analyses were performed using the HPLC. Van der Kamp et al. (1996) have noted that radial diffusion cells constructed with small reservoir volumes resulted in less precise analyses. In the van der Kamp study, five out of six radial diffusion cells experiments predicted a higher value for effective porosity than that of total porosity using Deuterium as a tracer, and only one out of six over-predicted using Cl or SO₄ as a tracer. Because, the effective porosity determined by model simulations, should be equal to or less than that of the total porosity, it is suggested that the experimental procedures used in this study lack sensitivity to distinguish between the effective and total porosity.

A comparison of effective porosity determined by model simulation, with that calculated using steady-state tracer concentrations is given in Tables 6 and 7. The effective porosity may be calculated using steady-state tracer concentration values using the following equation (Novakowski and van der Kamp, 1996):

$$\beta_1 = V_r / R \theta_e \gamma_r r_r$$

where β_1 is the dimensionless mixing coefficient calculated using the cell radius versus the radius of the reservoir and the equilibrium concentration at the end of the experiment (this value may also incorporate a correction in the equilibrium concentration to account for mass loss during sampling events), V_r is the reservoir volume, R is the dimensionless retardation factor (1.0 for a conservative tracer), θ_e is the effective porosity, γ_r is the cross-sectional area through which diffusion occurs, and r_r is the radius of the reservoir.

The calculated effective porosity corrected for mass loss (Table 6), from the forward radial diffusion experiments for Br, NO₂ and DFBA are, in general, lower by 0.5 to 1% than that of the model predicted porosity. For the reverse radial diffusion tests using Br tracer, approximately half of the calculated porosity using steady state concentrations are lower than the model predicted porosity, by 1 to 8% and the other tests are higher by <1%.

When the mass loss is not incorporated into the steady-state porosity calculations (Table 7) more than half of the values for the forward Br and DFBA radial diffusion tests over estimate the porosity determined using the model. Thus, calculated steady-state porosities are generally not in agreement with those predicted by the model calculations, or by gravimetric porosity measurements.

Effective diffusion coefficient

The effective diffusion coefficient is estimated from the diffusion process by the amount of curvature in the concentration versus time curves (Figures 2 a, b and c). Model predicted effective diffusion coefficients range from 0.01 to 0.65 cm²/d for the forward diffusion experiments using the Br tracer with an arithmetic mean of 0.15 cm²/d +/- 0.14 (excluding outlier data from OH3a, Table 8). This compares favorably to the reverse

radial diffusion Br experiments with a mean value of 0.175 cm²/d. Modeled predicted effective diffusion coefficients using DFBA tracer range from 0.01 to 0.98 cm²/d with an average of 0.21. The effective diffusion coefficient is a measurement of the rate at which diffusion will occur in the rock matrix and therefore is directly proportional to the size of the tracer particle. It is unlikely that Br, a small ion would have a lower effective diffusion coefficient than that of DFBA, a large molecule. However, data used to calculate the mean includes the first DFBA tracer experiments using Ion Chromatography (e.g. Cells G1, E1, E3, E2, and G3). This method was inadequate to analyze samples with high salinity and therefore curvature of the relative concentration with time plots was difficult to accurately define. Thus, analytical methods for DFBA detection were reverted to using HPLC instrumentation. When these data are excluded, mean values in the forward radial diffusion experiments for Br and DFBA are 0.16 cm²/d +/- 0.14 and 0.09 cm²/d +/- 0.05 respectively.

Accurate values of the effective-diffusion coefficients are necessary for the determination of a geometric factor (Table 9). The geometric factor is a property of the porous media and represents a quantitative measure of the difficult (or tortuous) path a molecule undergoes during diffusion into the matrix. The geometric factor is determined by the equation:

$$D^* = \tau D_0$$

where D^* is the effective diffusion coefficient, τ is the geometric factor ($0 < \tau < 1$), and D_0 is the free-water diffusion coefficient for the individual ion. The D_0 for Lissamine is estimated to be 4.5×10^{-9} m²/s (Novakowski and van der Kamp, 1996) by comparison to a similar compound, Uranine (Skagius and Neretnieks, 1986). Free-water diffusion coefficient for Br is 2.08×10^{-9} m²/s (Lide, 1992), 1.91×10^{-9} m²/s for NO₂ (Lide, 1992) and 7.6×10^{-9} m²/s for DFBA (Bowmans and Gibbens, 1996).

Since the geometric factor is a property of the matrix, comparison should be on an individual cell basis using the different tracers. Also, the geometric factor should not depend on the type of tracer used and thus calculated values for different diffusion

experiments performed on the same core sample should be similar. Percent differences were calculated using the difference of the two geometric factors determined for the same cell over the sum. The percent difference in the geometric factor for the forward Br compared to the forward NO₂ and also the reverse Br diffusion tests range from 1 to 36%. For the forward Br and DFBA tests (excluding tests whose DFBA analyses were performed by IC), percent differences are much larger, ranging from 15 to 83% with an average of ~30%. The large percent difference is directly related to the inaccuracies in the predicted effective diffusion coefficient. Thus, the diffusion coefficient determined by the current radial diffusion procedure is subject to a degree of error sufficient to prevent the accurate estimation of a geometric factor.

Conclusions

Current analytical procedures and experimental methods for the radial diffusion method can predict the total gravimetric porosity within a range of 1 to 2%. Although this error may be considered minor in some studies, it is too large to distinguish an effective porosity. Analytical procedures also lack adequate sensitivity to determine a precise effective diffusion coefficient. Errors in the effective diffusion coefficient are propagated in the calculation of the geometric factor.

The trial and error approach used in this study has determined that Lissamine FF does not behave conservatively in the environment imposed by the diffusion experiment. However, DFBA was found to be a good tracer in this rock type. Future investigations should explore the use of DFBA as a field tracer.

References

- Bowman, R.S., and Gibbens, J.F., 1992. Difluorobenzoates as non-reactive tracers in soil and groundwater. *Ground Water*, 30(1):8-14.
- Bickerton, G.S., 1997. Chemical and mineralogical composition of the Lockport and Rochester formations, Smithville, Ontario. Internal Report. NWRI Contribution No. 97-30.
- Langer, V., 1997. Resaturation and hydraulic conductivity of rock samples from the Lockport Formation at Smithville, southern Ontario, Canada. Unpublished report, National Water Research Institute, 8 p.
- Lide, D.R., 1992. *CRC Handbook of Chemistry and Physics*. 73rd edition. CRC Press, Ann Arbor.
- Novakowski, K.S. and van der Kamp, G., 1996. The radial diffusion method. 2. A semianalytical model for the determination of effective diffusion coefficients, porosity, and adsorption. *Water Resources Research*, 32(6): 1823-1830.
- Novakowski, K.S. and Lapcevic, P.A., 1994. Field measurement of radial solute transport in fractured rock. *Water Resources Research*, 30(1):37-44.
- Novakowski, K.S., Bickerton, G., and Lapcevic, P., 1999. Interpretation of injection-withdrawal tracer experiments conducted between two wells in a large single fracture. *Water Resources Research*, in submittal.
- Shackelford, C.D., Daniel, D.E. and Liljestrand, H.M., 1989. Diffusion of inorganic species in compacted clay soil. *Journal of Contaminant Hydrology*, 4:241-273.
- Skagius, K and Neretnieks, I., 1986. Porosities and diffusivities of some nonsorbing species in crystalline rocks. *Water Resources Research*, 22 (3): 389-398.
- Smart, P.L. and I.M.S. Laidlaw, 1977. An evaluation of some fluorescent dyes for water tracing. *WRR* 13(1): 15-33.
- van der Kamp, G., Van Stempvoort, D.R., and Wassenaar, L.I., 1996. The radial diffusion method. 1. Using intact cores to determine isotopic composition, chemistry, and effective porosities for groundwater aquitards. *Water Resources Research*, 32(6): 1815-1822.

Acknowledgments

The assistance of Susan Brown and Kelly Millar in the lab and advice from Suzanne Lesage are gratefully appreciated.

Table 1: Cell locations and dimensions

Cell name	Formation	Borehole Location	Date Started	Date Ended	Sample Interval (fbgs - along core)	Cell Height (cm)	Cell Radius (cm)	Reservoir Radius (cm)
Cell 1	Goat Island	BH54A	28/4/97	26/8/97	112.50	8.81	2.25	0.64
Cell 9	Vinemount	BH59	28/4/97	26/8/97	114.25	11.48	2.25	0.66
Cell 10	Gasport	BH59	28/4/97	26/8/97	136.58	6.85	2.25	0.65
Cell D	Gasport	BH54B	28/4/97	26/8/97	124.42	9.42	2.24	0.61
Cell OH3a	Ont. Hydro		14/4/97	9/6/97	-	6.48	3.16	0.64
Cell C	Goat Island	BH54B	28/4/97	9/6/97	83.58	9.54	2.24	0.63
control 1	Stainless Steel		14/4/97	24/4/97	-	7.00	2.25	0.40
Cell 6	Eramosa	BH58	20/10/97	29/01/98	71.25	10.12	2.25	0.63
Cell A	Vinemount	BH64	20/10/97	29/01/98	121.75	13.17	2.25	0.64
Cell B	Vinemount	BH64	20/10/97	29/01/98	122.33	11.53	2.24	0.64
Cell V1	Vinemount	BH54A	20/10/97	29/01/98	94.42	10.16	2.25	0.63
Cell G1	Gasport	BH64	16/02/98	13/02/98	110.75	11.94	2.25	0.62
Cell E1	Eramosa	BH64	16/02/98	13/02/98	15.00	13.99	2.25	0.64
Cell E3	Eramosa	BH64	16/02/98	13/02/98	27.17	10.16	2.25	0.63
Cell E2	Eramosa	BH64	16/02/98	13/02/98	26.58	14.11	2.25	0.63
Cell G3	Gasport	BH64	16/02/98	13/02/98	121.83	12.89	2.25	0.62
Control 2	Stainless Steel		16/02/98	13/02/98	-	7.00	2.25	0.63
Cell ER1	Eramosa	BH64	22/04/98	2/6/98	17.16	10.55	2.25	0.63
Cell V2-1	Vinemount	BH64	22/04/98	2/6/98	55.67	12.16	2.25	0.63
Cell GA-1	Gasport	BH64	22/04/98	2/6/98	112.00	11.97	2.25	0.63
Cell E2-3	Eramosa	BH64	22/04/98	2/6/98	35.75	10.47	2.24	0.63
Cell E2-2	Eramosa	BH64	22/04/98	2/6/98	25.42	11.66	2.25	0.64
Cell GA-2	Gasport	BH64	22/04/98	2/6/98	110.75	12.45	2.25	0.63
Cell GI-1	Goat Island	BH64	22/04/98	2/6/98	100.00	12.13	2.24	0.63
Control 2	Stainless Steel		22/04/98	2/6/98	-	7.00	2.25	0.63
Cell jun4v21	Vinemount	BH64	27/06/98	16/09/98	54.75	11.85	2.24	0.64
Cell jun4e1	Eramosa	BH64	27/06/98	16/09/98	27.75	12.15	2.19	0.63
Cell jun4vi1	Vinemount	BH64	27/06/98	16/09/98	74.75	12.15	2.37	0.64
Cell jun4e2	Eramosa	BH64	27/06/98	16/09/98	37.75	11.66	2.25	0.63
Cell jun5gi1	Goat Island	BH64	27/06/98	16/09/98	102.00	11.53	2.24	0.63
Cell jun5r1	Rochester	BH64	27/06/98	16/09/98	133.00	13.25	2.25	0.63
Cell jun5gi2	Goat Island	BH64	27/06/98	16/09/98	95.33	12.50	2.26	0.63
Cell jun5ga1	Gasport	BH64	27/06/98	16/09/98	112.58	12.22	2.25	0.61
Control 2	Stainless Steel		27/06/98	16/09/98	-	7.00	2.25	0.63

Table 2: Physical description of samples used for diffusion cells

Sample	Formation	Description
cell 1	Goat Island	brown/gray, fine grained dolostone, small vugs (1 - 2 cm diameter), discontinuous, stylolite (~1 mm thick)
cell 9	Vinemount	brown/gray, fine grained, massive dolostone, contains some gypsum (1%)
cell 10	Gasport	light gray, medium grained dolostone, highly fossilized, contains some gypsum nodules.
cell D	Gasport	light gray, medium grained, dolostone, fossilized, large amounts of gypsum infilling features (~40 %)
cell OH3a	-	light brown, fine grained, limestone with mm scale bedding.
Cell C	Goat Island	light brown, fine to medium grained dolostone
Cell 6	Eramosa	brown gray, fine-med grained dolostone, massive, contains pyrite
Cell A	Vinemount	dark gray, fine grained dolostone, gypsum filled vugs, dissolution features
Cell B	Vinemount	dark gray, fine grained dolostone, gypsum filled vugs, dissolution features, cm scale bedding
Cell V1	Vinemount	brown gray, fine grained dolostone, massive, calcite and gypsum filled vugs
Cell G1	Gasport	light gray, fine grained dolostone, pits and fossils
Cell E1	Eramosa	brown gray, fine grained dolostone, mm scale beds, stylolite, dissolution features, pyrite grains
Cell E3	Eramosa	brown gray, fine-med grained dolostone, cm scale beds, pits, pyrite grains
Cell E2	Eramosa	brown gray, fine-med grained dolostone, cm scale bed, pyrite grains
Cell G3	Gasport	light gray, fine-med grained dolostone, slightly bedded, fossils
Cell ER1	Eramosa	brown gray, fine grained dolostone, gypsum filled vugs, pyrite grains
Cell V2-1	Vinemount	brown gray, fine grained dolostone, mm scale bedding, stylolites
Cell GA-1	Gasport	light gray, med-large grained dolostone, minor bedding on mm scale, minor vugs, fossils
Cell E2-3	Eramosa	brown gray, fine grained dolostone, mm scale bedding , vugs, pyrite grains
Cell E2-2	Eramosa	brown gray, med grained dolostone, cm bed
Cell GA-2	Gasport	light gray, med-large grained dolostone, minor bedding on mm scale, fossils

Table 2: Continued

Sample	Formation	Description
Cell GI-1	Goat Island	dark gray, fine-med grained dolostone, minor bedding
Cell jun4v21	Vinemount	brown gray, fine grained dolostone, small vugs
Cell jun4e1	Eramosa	gray, fine-med grained dolostone, cm scale beds, infilled calcite vug
Cell jun4vi1	Vinemount	gray, fine grained dolostone, mm scale beds, gypsum filled vugs
Cell jun4e2	Eramosa	brown gray, fine-med grained dolostone, mm scale bedding, dissolution features
Cell jun5gi1	Goat Island	gray, fine grained dolostone, stylolite, gypsum filled vugs
Cell jun5r1	Rochester	gray, fine grained dolostone, cm and mm scale beds
Cell jun5gi2	Goat Island	brown gray, fine grained dolostone, mm scale beds
Cell jun5ga1	Gasport	light gray, fine grained dolostone, mm scale beds, fossils

Table 3: Measured reservoir volume for each test (mL)

Cell Name	Forward Lissamine	Reverse Lissamine	Forward Bromide	Reverse Bromide	Forward Nitrite	Forward dfba
Cell 1	11.5	11.5	11.5	11.5		
Cell 9	15	14.7	15	14.7		
Cell 10	8.8	8.8	8.8	8.8		
Cell D	11.6	11.9	11.6	11.9		
Cell OH3a	9		9			
Cell C		12.1				
control 1	3.8					
Cell 6	12.6	12.8	12.6	12.8	12.8	11.8
Cell A	16.9	16.6	16.9	16.6	16.6	
Cell B	12.9	14.6	12.9	14.6	14.6	
Cell V1	13.2	13.3	13.2	13.3	13.3	
Cell G1			14.6			14.6
Cell E1	17.1		17.1			
Cell E3			17.7			17.7
Cell E2			15.3			15.3
Cell G3			16.7			16.7
Control 2			9			9
Cell ER1			13.5			13.5
Cell V2-1			16			16
Cell GA-1			14.6			14.6
Cell E2-3			13.2			13.2
Cell E2-2			14.7			14.7
Cell GA-2			15			15
Cell GI-1			15.2			15.2
Control 2			8.2			8.2
Cell jun4v21			13.43			13.43
Cell jun4e1			15.03			15.03
Cell jun4vi1			14.88			14.88
Cell jun4e2			14.39			14.39
Cell jun5gi1			14.56			14.56
Cell jun5r1			16.23			16.23
Cell jun5gi2			14.96			14.96
Cell jun5ga1			15.22			15.22
Control 2			8.59			8.59

Table 4: Tracer type used during radial diffusion experiments

Cell Name	Forward Lissamine	Reverse Lissamine	Forward Bromide	Reverse Bromide	Forward Nitrite	Forward dfba
Cell 1	x	x	x	x		
Cell 9	x	x	x	x		
Cell 10	x	x	x	x		
Cell D	x	x	x	x		
Cell OH3a	x		x			
Cell C		x				
control 1	x					
Cell 6	x	x	x	x	x	x
Cell A	x	x	x	x	x	
Cell B	x	x	x	x	x	
Cell V1	x	x	x	x	x	
Cell G1			x			x
Cell E1	x		x			
Cell E3			x			x
Cell E2			x			x
Cell G3			x			x
Control 2			x			x
Cell ER1			x			x
Cell V2-1			x			x
Cell GA-1			x			x
Cell E2-3			x			x
Cell E2-2			x			x
Cell GA-2			x			x
Cell G1-1			x			x
Control 2			x			x
Cell jun4v21			x			x
Cell jun4e1			x			x
Cell jun4vi1			x			x
Cell jun4e2			x			x
Cell jun5gi1			x			x
Cell jun5r1			x			x
Cell jun5gi2			x			x
Cell jun5ga1			x			x
Control 2			x			x

Table 5: Model predicted effective porosity (Retardation = 1) and gravimetric porosity results in %

Cell Name	Forward Lissamine	Reverse Lissamine	Forward Bromide	Reverse Bromide	Forward Nitrite	Forward dfba	Gravimetric Porosity
Cell 1	49	9	11	11			8.2
Cell 9	47	9	8	10			10.2
Cell 10	22	15.4	11	17.9			15.7
Cell D	4	1.2	2.5	4.6			7.5
Cell OH3a	11		12				20
Cell C		3					6.5
control 1	1.5						
Cell 6	42	9	9	7.5	9	12	7.8
Cell A	58	10.6	5	3	5		3.7
Cell B	58	10.6	6	3	5		3.2
Cell V1	30	4	4	2	6.4		2.6
Cell G1			9.4			5.8	5.8
Cell E1			9.4				5
Cell E3			10.6			7	8.6
Cell E2			8.2			5.8	4.1
Cell G3			9.4			8.2	6.8
Control 2			4.6			4.6	-
Cell ER1			4.6			4.6	4.5
Cell V2-1			5.8			13	5.2
Cell GA-1			8.2			8.2	8.9
Cell E2-3			8.2			9.4	7.8
Cell E2-2			5.8			4.6	5.7
Cell GA-2			4.6			4.6	6
Cell GI-1			11.8			10.6	11.4
Control 2			1			1	-
Cell jun4v21			7			5.82	6.5
Cell jun4e1			9.4			8.22	7.6
Cell jun4vi1			5.8			4.61	5.5
Cell jun4e2			7			5.82	5.5
Cell jun5gi1			9.4			9.4	8.1
Cell jun5r1			8.2			8.2	7.3
Cell jun5gi2			9.4			9.4	8.2
Cell jun5ga1			8.2			8.2	6.8
Control 2			1			1	-

Table 6: Calculated porosity from steady-state concentrations using $B = V_r/\theta_c \gamma_{rr}$; corrected for mass loss due to sampling

Cell Name	Forward Lissamine	Reverse Lissamine	Forward Bromide	Reverse Bromide	Forward Nitrite	Forward dfba
Cell 1	40.7	11.2	9.9	9.3		
Cell 9	42.5	10.2	7.3	6.9		
Cell 10	19.7	23.4	10	9.2		
Cell D	3.1	1.4	1.6	1.3		
Cell OH3a	10.4		10.4			
Cell C		3.01				
control 1						
Cell 6	31.4	10.3	8	8.3	7.7	
Cell A	27.8	12.1	4.5	3.2	4.7	
Cell B	30.6	11.2	5.4	2.9	4.2	
Cell V1	12.7	4.3	3.6	2.3	5.6	
Cell G1			5.5			7.7
Cell E1			7.8			5.8
Cell E3			8.7			8.7
Cell E2			5.1			4.9
Cell G3			8			8
Control 2			1.9			3.9
Cell ER1			4			3.9
Cell V2-1			5.1			4.2
Cell GA-1			7.5			7.2
Cell E2-3			7.3			8.5
Cell E2-2			5.3			4.1
Cell GA-2			4.2			3.8
Cell GI-1			10.8			10
Control 2			0			0
Cell jun4v21			6.4			5.1
Cell jun4e1			8.6			7.2
Cell jun4vi1			5.3			4.1
Cell jun4e2			6.2			5.1
Cell jun5gi1			8.7			8.3
Cell jun5r1			7.4			6.7
Cell jun5gi2			8.4			8.4
Cell jun5ga1			7.5			6.3
Control 2			0.4			0.6

Table 7: Calculated porosity from steady-state concentrations using $B = V_r/\theta_e \gamma_{r,r}$; not corrected for mass loss due to sampling

Cell Name	Forward Lissamine	Reverse Lissamine	Forward Bromide	Reverse Bromide	Forward Nitrite	Forward dfba
Cell 1	49.2	9	12.4	11		
Cell 9	49.2	9	9	10.1		
Cell 10	26.2	15.8	13.4	18.1		
Cell D	4.7	1.2	2.6	3.8		
Cell OH3a	13.6		13.6			
Cell C		3.01				
control 1						
Cell 6	36.3	8.5	10	7	9.6	12
Cell A	31.2	10.3	5.6	2.9	5.6	
Cell B	35.2	9.1	6.9	2.6	5.6	
Cell V1	14.5	3.6	4.8	1.9	6.7	
Cell G1			6.3			8.7
Cell E1			8.7			6.5
Cell E3			9.7			9.7
Cell E2			5.8			5.6
Cell G3			8.9			8.9
Control 2			2.9			5.1
Cell ER1			5.3			5.1
Cell V2-1			6.3			5.2
Cell GA-1			8.9			8.6
Cell E2-3			8.9			10.2
Cell E2-2			6.5			5.3
Cell GA-2			5.2			4.8
Cell GI-1			12.5			11.5
Control 2			1			1.3
Cell jun4v21			7.8			6.4
Cell jun4e1			10.2			8.6
Cell jun4vi1			6.4			5.2
Cell jun4e2			7.5			6.4
Cell jun5gi1			10.2			9.8
Cell jun5r1			8.7			8.1
Cell jun5gi2			9.9			9.9
Cell jun5ga1			8.8			7.5
Control 2			1.7			2

Table 8: Model predicted effective diffusion coefficients (Retardation = 1); results in cm²/d

Cell Name	Forward Lissamine	Reverse Lissamine	Forward Bromide	Reverse Bromide	Forward Nitrite	Forward dfba
Cell 1	0.04	0.2	0.18	0.1		
Cell 9	0.04	0.2	0.17	0.17		
Cell 10	0.24	0.18	0.58	0.34		
Cell D	0.09	0.3	0.28	0.05		
Cell OH3a	0.46		1.42			
Cell C		1				
control 1	1					
Cell 6	0.02	0.15	0.14	0.11	0.11	0.09
Cell A	0.01	0.06	0.13	0.11	0.1	
Cell B	0.01	0.06	0.16	0.15	0.09	
Cell V1	0.01	0.06	0.19	0.37	0.08	
Cell G1*			0.04			0.57
Cell E1			0.09			
Cell E3*			0.04			0.58
Cell E2*			0.024			0.98
Cell G3*			0.08			0.22
Control 2*			0.03			0.95
Cell ER1			0.14			0.07
Cell V2-1			0.08			0.012
Cell GA-1			0.16			0.07
Cell E2-3			0.65			0.2
Cell E2-2			0.15			0.15
Cell GA-2			0.12			0.06
Cell GI-1			0.24			0.12
Control 2			0.01			0.04
Cell jun4v21			0.1			0.09
Cell jun4e1			0.09			0.07
Cell jun4vi1			0.15			0.18
Cell jun4e2			0.09			0.09
Cell jun5gi1			0.11			0.06
Cell jun5r1			0.1			0.05
Cell jun5gi2			0.18			0.1
Cell jun5ga1			0.08			0.04
Control 2			0.04			0.01

* DFBA analyses determined using IC, subject to error

Table 9: Calculated geometric factors. Do (Lissamine) = $4.5 \times 10^{-9} \text{ m}^2/\text{s}$, Do(Br) = $2.08 \times 10^{-9} \text{ m}^2/\text{s}$, Do(NO₂) = $1.91 \times 10^{-9} \text{ m}^2/\text{s}$ and Do(DFBA) = $7.6 \times 10^{-10} \text{ m}^2/\text{s}$

Cell Name	Forward Lissamine	Reverse Lissamine	Forward Bromide	Reverse Bromide	Forward Nitrite	Forward dfba
Cell 1	0.010	0.051	0.100	0.061		
Cell 9	0.010	0.051	0.095	0.103		
Cell 10	0.062	0.046	0.323	0.206		
Cell D	0.023	0.077	0.156	0.030		
Cell OH3a	0.118		0.790			
Cell C		0.257				
control 1	0.257					
Cell 6	0.005	0.039	0.078	0.067	0.067	0.137
Cell A	0.003	0.015	0.072	0.067	0.100	
Cell B	0.003	0.015	0.089	0.091	0.090	
Cell V1	0.003	0.015	0.106	0.224	0.080	
Cell G1*			0.022			0.868
Cell E1			0.050			
Cell E3*			0.022			0.883
Cell E2*			0.013			1.492
Cell G3*			0.045			0.335
Control 2*			0.017			1.446
Cell ER1			0.078			0.107
Cell V2-1			0.045			0.018
Cell GA-1			0.089			0.107
Cell E2-3			0.362			0.304
Cell E2-2			0.083			0.228
Cell GA-2			0.067			0.091
Cell GI-1			0.134			0.183
Control 2			0.006			0.061
Cell jun4v21			0.056			0.137
Cell jun4e1			0.050			0.107
Cell jun4vi1			0.083			0.274
Cell jun4e2			0.050			0.137
Cell jun5gi1			0.061			0.091
Cell jun5r1			0.056			0.076
Cell jun5gi2			0.100			0.152
Cell jun5ga1			0.045			0.061
Control 2			0.022			0.015

* DFBA analyses determined using IC, subject to error

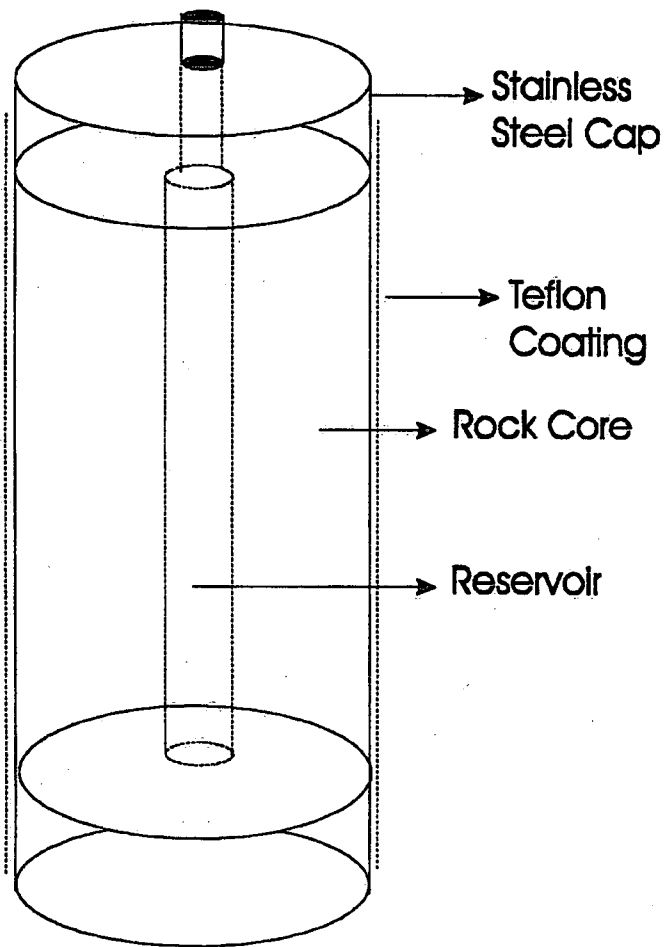


Figure 1: Diagram of a radial diffusion cell

Figure 2a: Forward diffusion experimental and simulated concentration curves: Lissamine and Bromide

April 1997 Cells

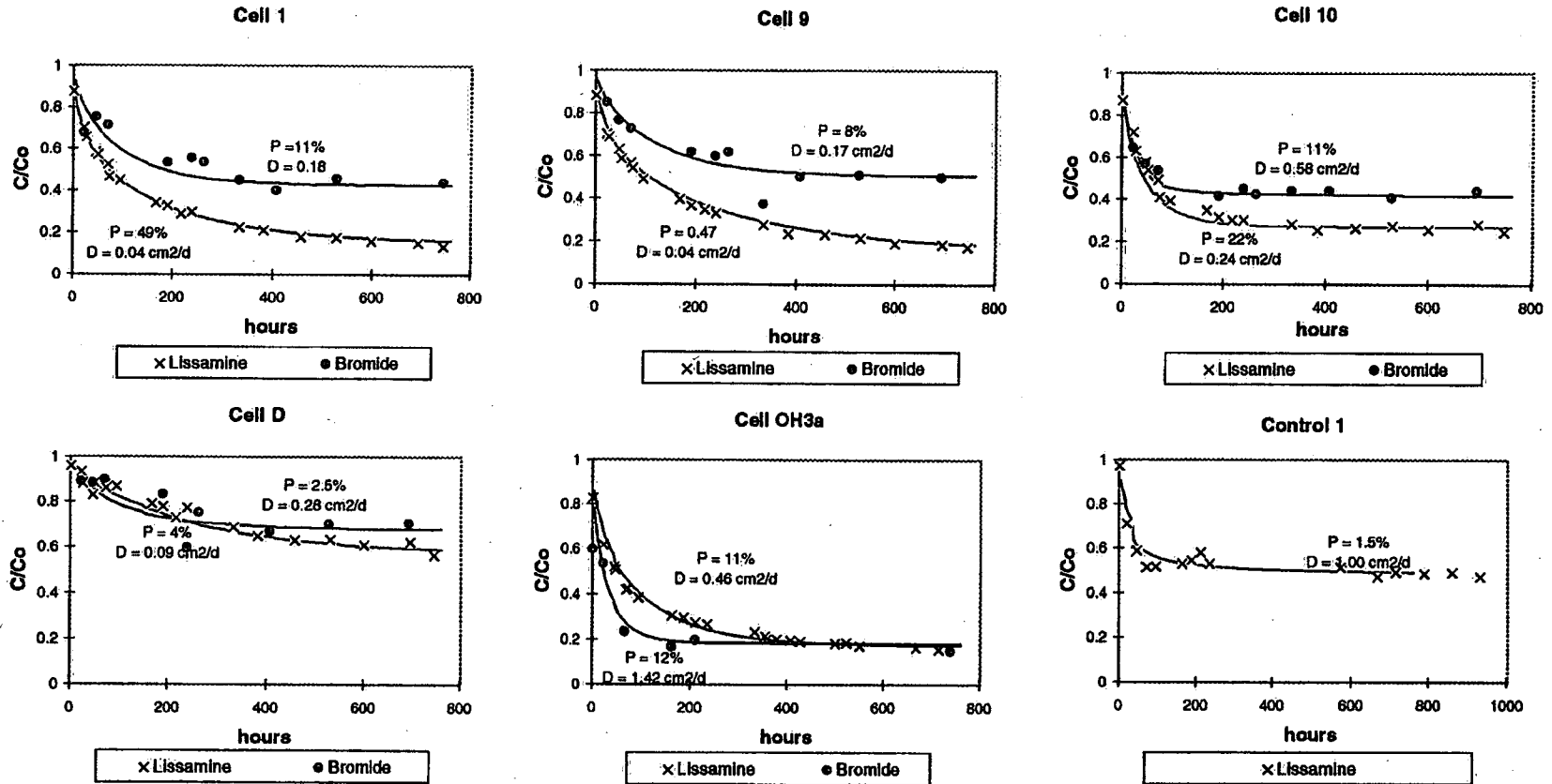


Figure 2a: Continued

June 1997 cells

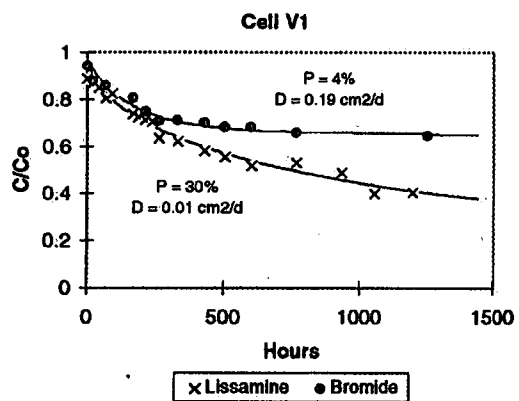
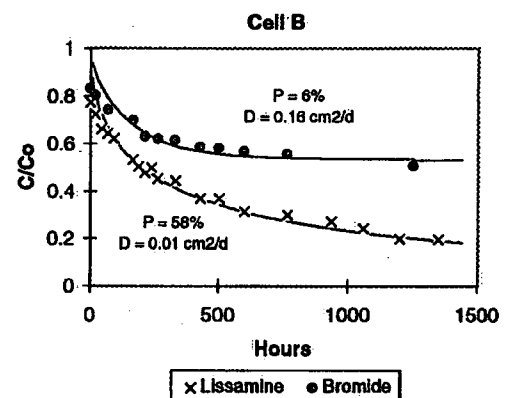
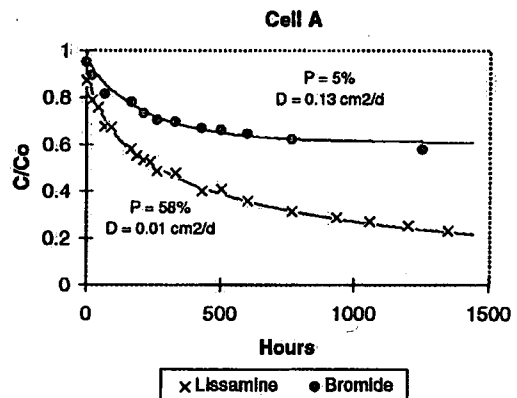
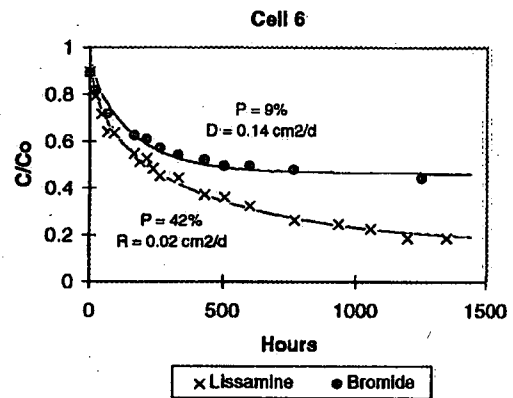


Figure 2a: Continued

March 1998 Cells

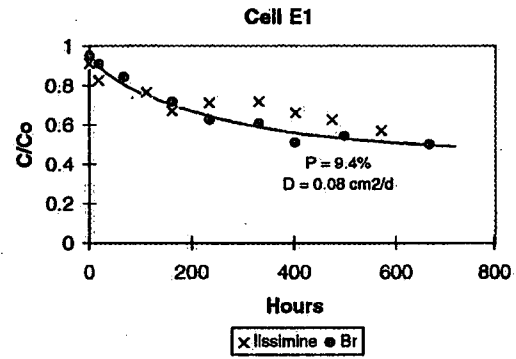


Figure 2b: Forward diffusion experimental and simulated concentration curves: Bromide and DFBA

March 1998 cells

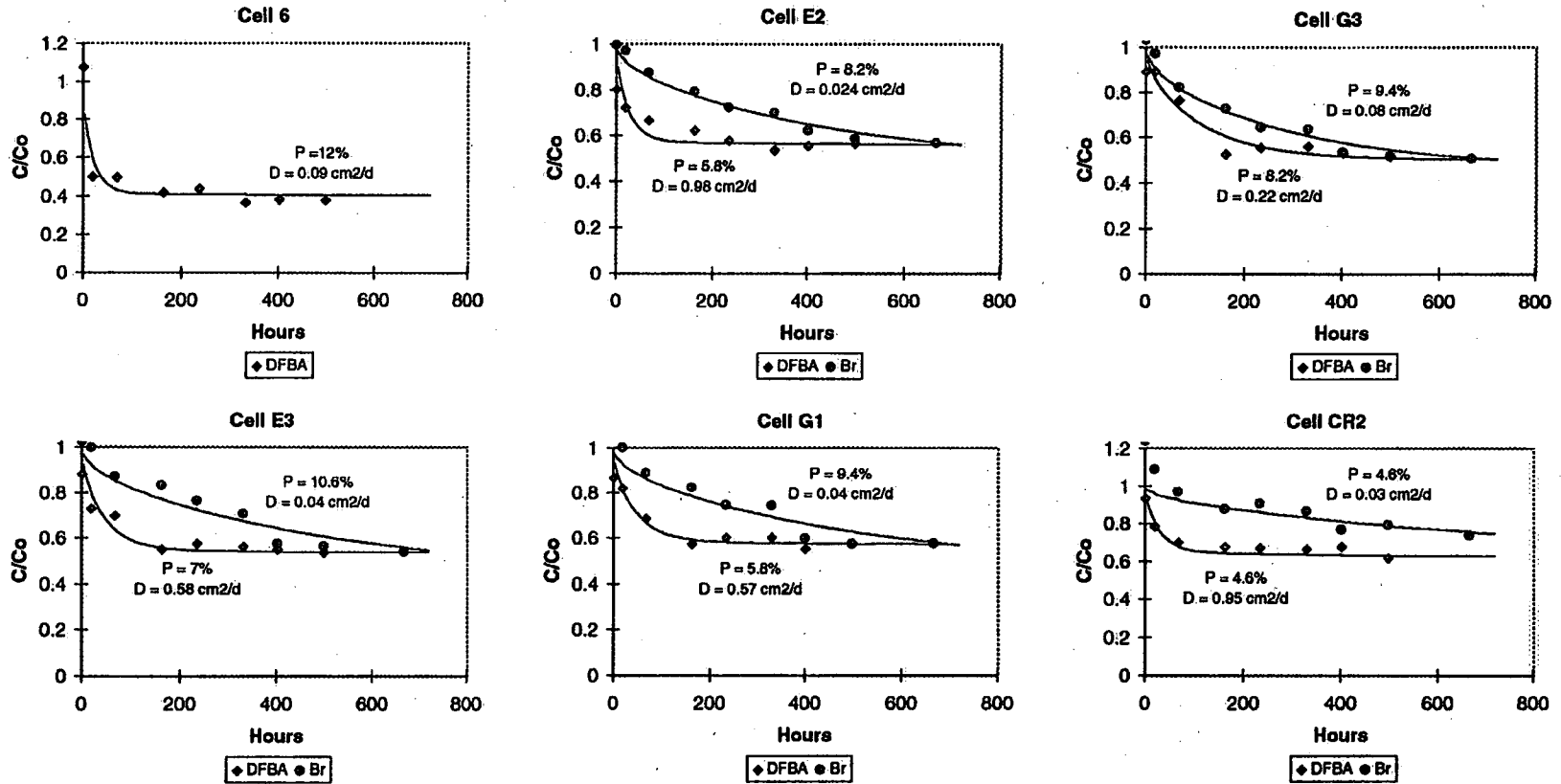


Figure 2b: Continued

April 1998 cells

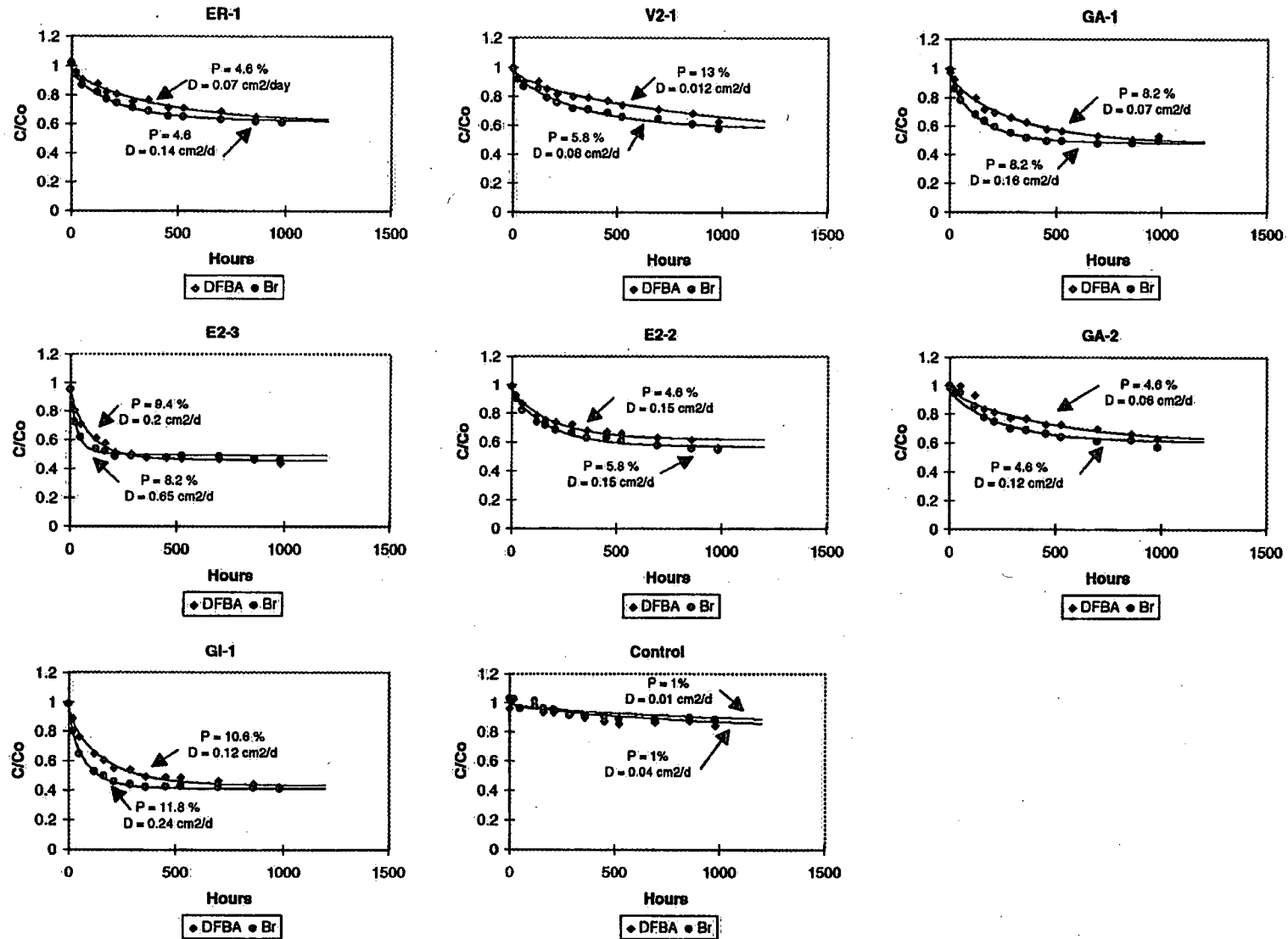


Figure 2b: Continued

July 1998 cells

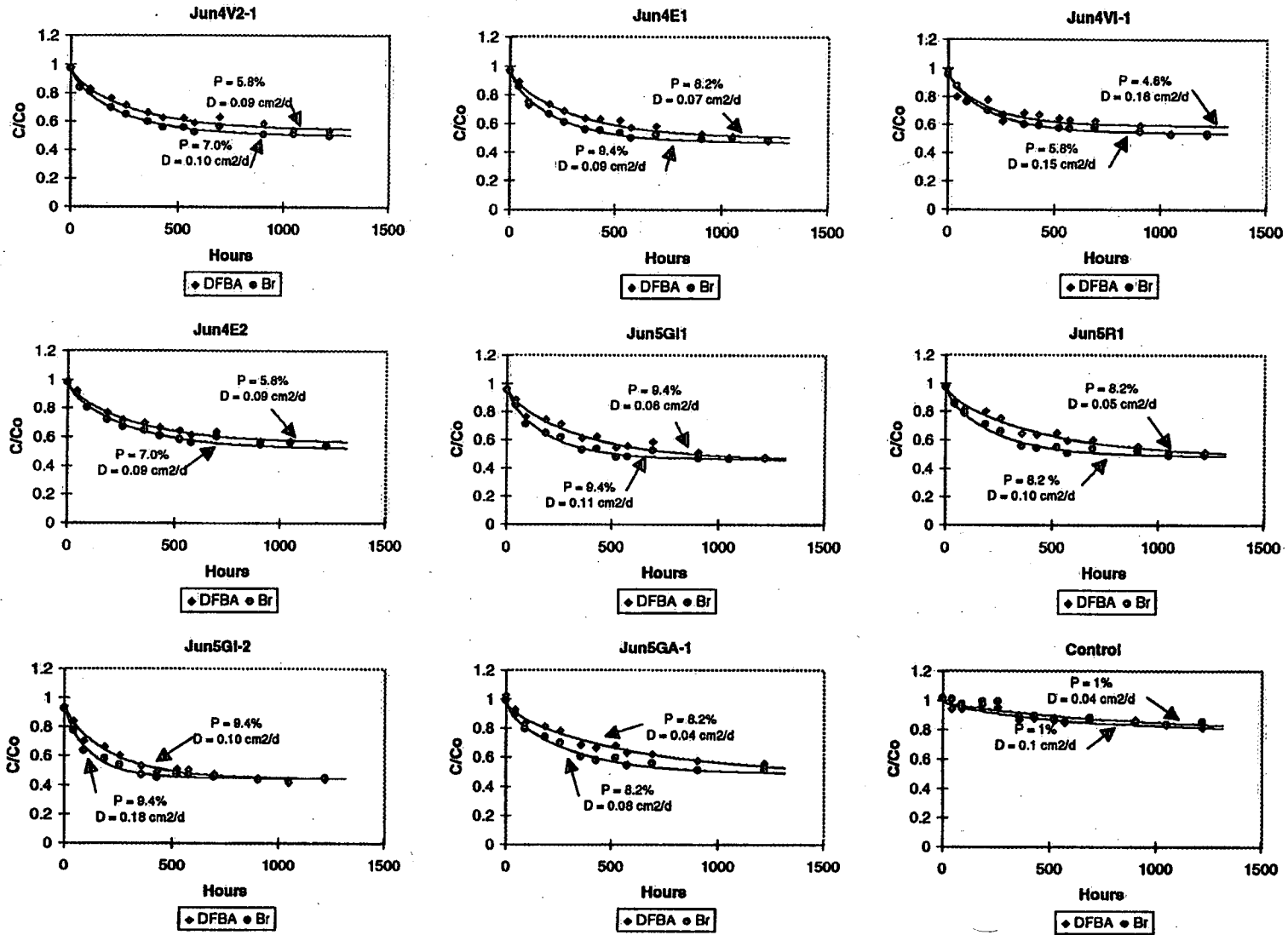


Figure 2c: Forward diffusion experimental and simulated concentration curves: Nitrite

June 1997 Cells

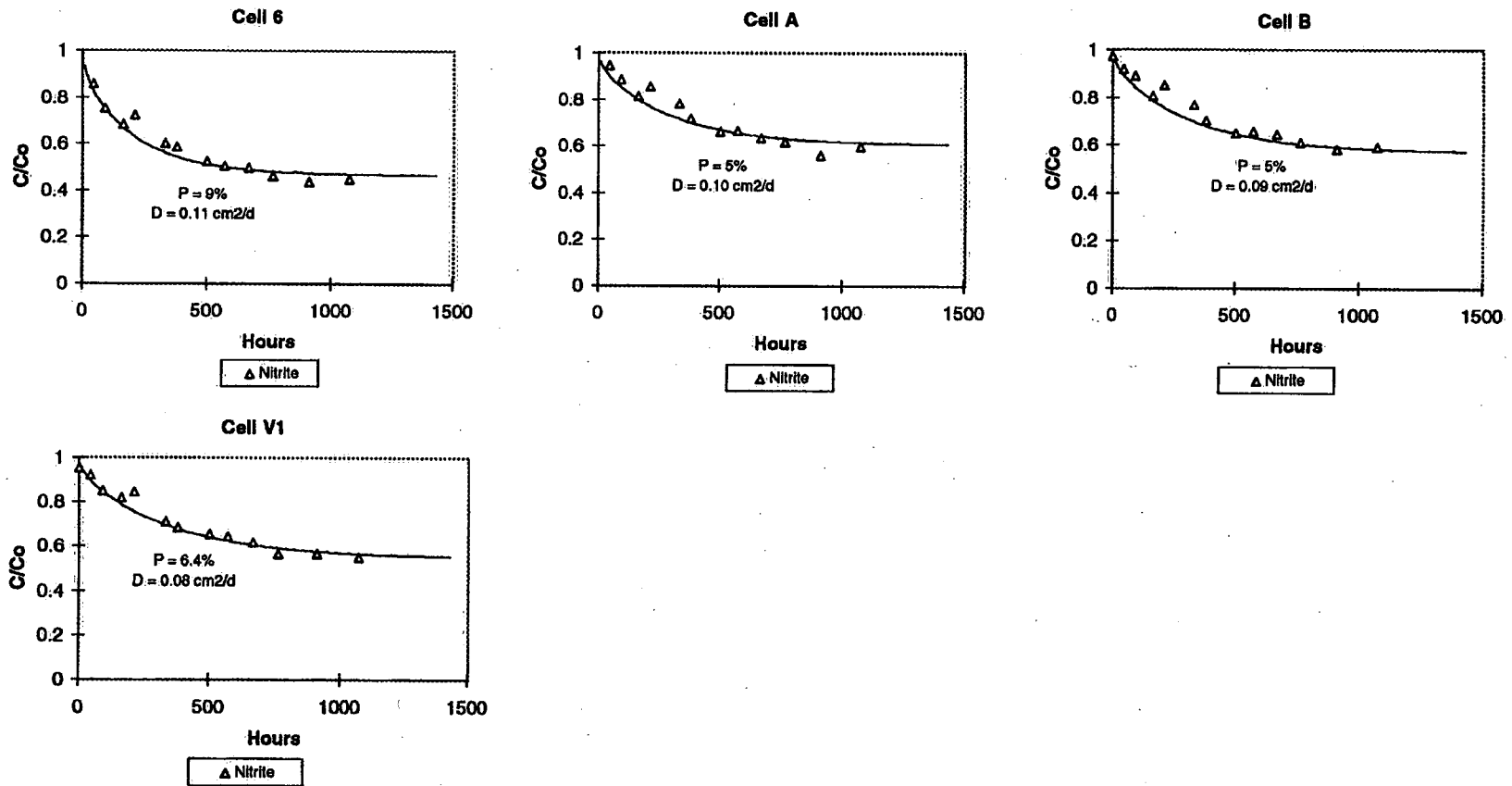


Figure 2d: Reverse diffusion experimental and simulated concentration curves: Lissamine and Bromide

April 1997 cells

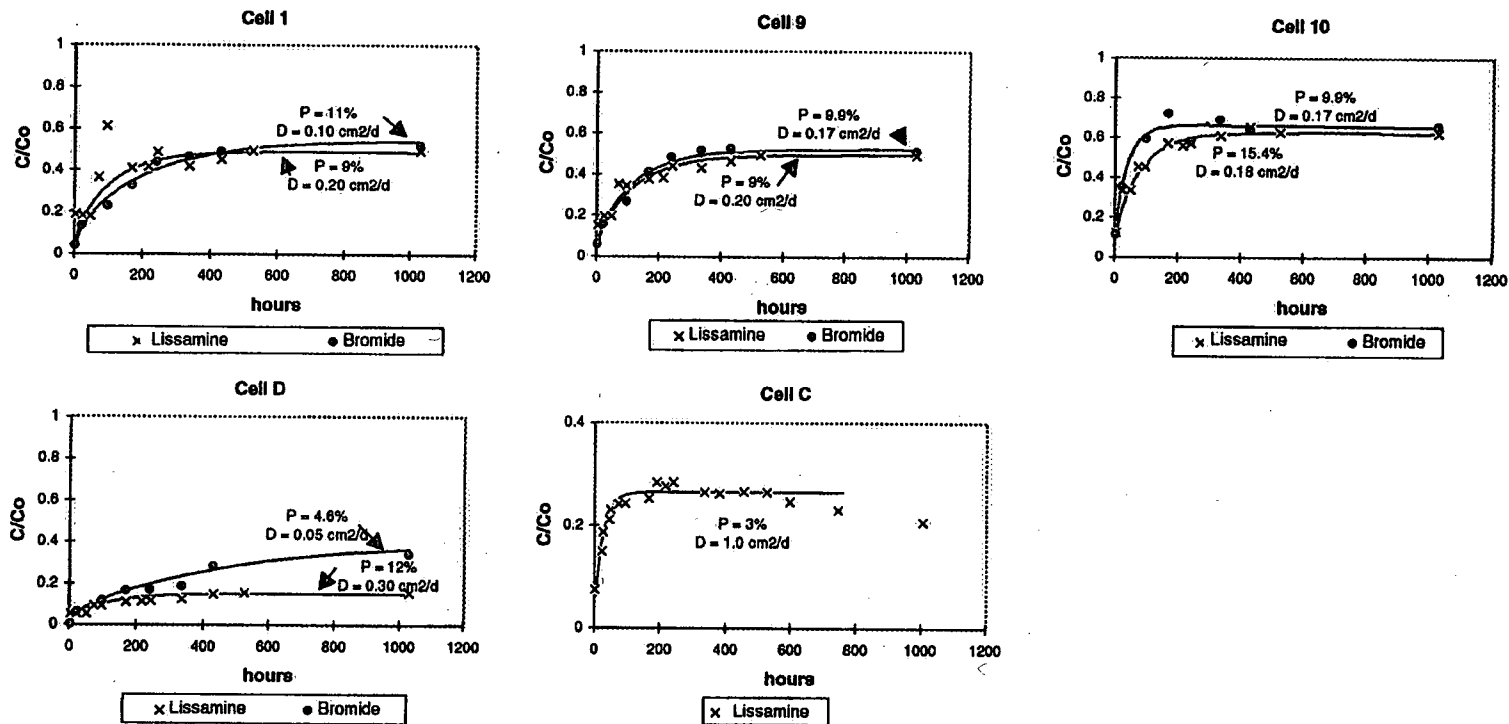
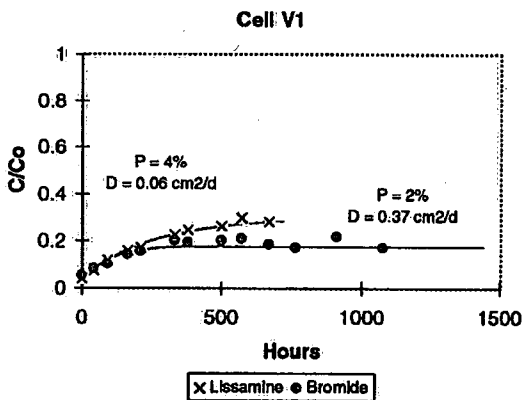
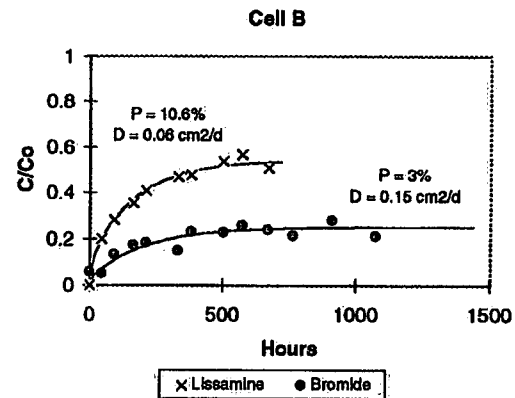
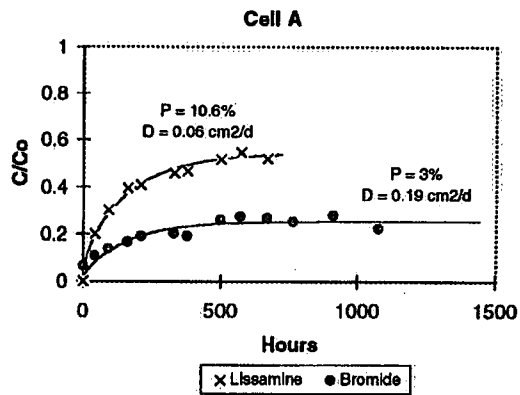
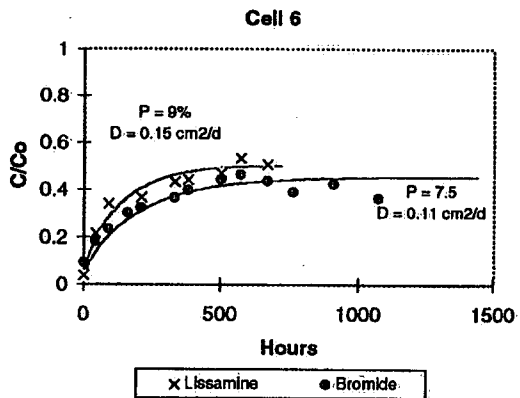


Figure 2d: Continued

June 1997 cells



APPENDIX A

Table A1: Experimental data for forward radial diffusion experiments: Lissamine

April 1997 cells

Cell 1		cell 9		cell 10		cell D		OH3a		Control	
Time (hr)	C/Co	Time (hr)	C/Co	Time (hr)	C/Co	Time (hr)	C/Co	Time (hr)	C/Co	Time (hr)	C/Co
1.50	0.88	1.50	0.88	1.50	0.87	1.50	0.96	1.47	0.83	2.13	0.97
22.67	0.70	22.72	0.70	22.62	0.72	22.70	0.93	22.60	0.62	21.05	0.71
26.93	0.66	27.00	0.69	26.92	0.63	27.00	0.88	44.45	0.52	44.58	0.58
46.75	0.58	46.85	0.63	46.85	0.58	46.92	0.83	47.25	0.51	47.47	0.59
50.88	0.57	50.97	0.58	50.88	0.54	50.93	0.88	69.08	0.42	69.20	0.51
70.70	0.52	70.77	0.57	70.68	0.49	70.67	0.88	72.63	0.42	72.72	0.51
73.92	0.46	74.00	0.54	73.88	0.41	73.78	0.86	94.50	0.38	95.23	0.52
95.03	0.45	94.95	0.49	94.83	0.39	94.75	0.87	163.00	0.30	163.80	0.53
167.58	0.34	167.50	0.39	167.33	0.35	167.27	0.79	187.63	0.29	187.73	0.54
190.88	0.33	190.83	0.37	190.72	0.31	190.65	0.78	211.50	0.27	211.63	0.58
217.67	0.29	217.57	0.35	217.37	0.30	217.38	0.73	235.55	0.26	235.67	0.53
239.83	0.29	239.75	0.33	239.55	0.30	239.53	0.77	333.76	0.23	572.97	0.51
335.53	0.22	335.42	0.27	335.30	0.28	335.20	0.69	355.65	0.21	668.68	0.47
382.58	0.21	384.50	0.23	384.38	0.25	384.28	0.65	359.01	0.20	715.80	0.49
455.82	0.18	457.68	0.23	457.57	0.26	457.50	0.63	379.90	0.20	788.97	0.49
527.75	0.18	529.63	0.22	529.50	0.27	529.45	0.63	406.97	0.19	860.97	0.49
598.30	0.16	600.23	0.19	600.08	0.26	600.03	0.61	427.70	0.19	931.48	0.47
694.00	0.15	695.92	0.18	695.78	0.28	695.70	0.62	500.38	0.18	1287.24	0.47
746.02	0.13	745.92	0.17	745.78	0.25	745.87	0.56	523.80	0.18		
1006.62	0.12	1006.52	0.14	1006.38	0.27	1006.32	0.55	550.58	0.17		
1343.35	0.11	1343.38	0.14	1343.41	0.29	1343.43	0.54	669.30	0.16		
								716.41	0.16		
								789.60	0.16		
								861.65	0.16		
								932.10	0.14		
								1287.20	0.14		

June 1997 cells

Cell 8		Cell A		Cell B		Cell V1	
Time (hr)	C/Co	Time (hr)	C/Co	Time (hr)	C/Co	Time (hr)	C/Co
0.58	0.90	0.47	0.87	0.35	0.77	0.93	0.89
20.25	0.79	20.15	0.79	20.03	0.72	20.60	0.87
43.63	0.72	43.52	0.76	43.40	0.66	43.97	0.85
67.91	0.64	67.80	0.68	67.68	0.64	68.23	0.81
91.90	0.64	91.80	0.67	91.72	0.62	92.27	0.82
167.67	0.55	167.55	0.58	167.43	0.53	168.03	0.74
188.07	0.51	187.95	0.55	187.95	0.50	188.50	0.72
213.70	0.53	213.67	0.53	213.55	0.48	214.15	0.71
238.42	0.48	238.35	0.53	238.23	0.50	238.78	0.71
264.48	0.45	264.42	0.49	264.30	0.45	264.85	0.63
334.15	0.44	334.08	0.48	333.97	0.44	334.53	0.62
430.48	0.37	430.42	0.40	430.30	0.37	430.85	0.58
503.47	0.36	503.40	0.41	503.30	0.37	503.85	0.56
598.93	0.32	599.08	0.36	599.20	0.31	599.75	0.52
766.80	0.26	766.73	0.31	766.42	0.30	767.17	0.53
934.20	0.25	934.10	0.29	934.00	0.27	934.60	0.49
1057.90	0.23	1057.00	0.27	1058.40	0.24	1057.00	0.40
1198.18	0.19	1198.12	0.25	1198.00	0.20	1198.55	0.40
1348.10	0.19	1348.03	0.23	1347.92	0.20		

March 1998 cells

Cell E1	
Time (hr)	C/Co
0.28	0.91
19.10	0.82
113.05	0.77
162.30	0.67
234.53	0.71
330.50	0.72
402.00	0.66
474.25	0.63
571.08	0.57

Table A2: Experimental data for forward radial diffusion experiments: Bromide

April 1997 cells

cell 1		cell 9		cell 10		cell D		OH3a	
Time (hr)	C/Co	Time (hr)	C/Co	Time (hr)	C/Co	Time (hr)	C/Co	Time (hr)	C/Co
22.58	0.68	22.75	0.85	22.75	0.64	22.75	0.89	1.47	0.60
47.08	0.75	47.08	0.78	47.18	0.57	47.18	0.88	22.60	0.53
70.62	0.71	70.62	0.72	70.62	0.54	70.62	0.90	66.32	0.23
190.50	0.53	190.50	0.62	190.50	0.42	190.50	0.83	163.65	0.17
239.42	0.56	239.50	0.60	239.53	0.45	239.58	0.60	211.72	0.19
264.75	0.54	264.75	0.62	264.75	0.42	264.75	0.75	740.80	0.15
335.20	0.45	335.20	0.37	335.25	0.44	407.42	0.67		
407.15	0.40	407.33	0.50	407.42	0.44	527.50	0.70		
527.23	0.46	527.33	0.51	527.50	0.41	693.83	0.70		
693.57	0.44	693.67	0.50	693.83	0.44				

June 1997 cells

Cell 6		Cell A		Cell B		Cell V1	
Time (hr)	C/Co	Time (hr)	C/Co	Time (hr)	C/Co	Time (hr)	C/Co
1.25	0.89	1.08	0.95	0.92	0.83	1.42	0.94
21.83	0.81	21.67	0.89	21.50	0.80	22.00	0.88
69.25	0.72	69.08	0.82	68.92	0.74	69.42	0.86
169.00	0.62	168.83	0.78	168.67	0.70	169.17	0.80
215.33	0.61	215.17	0.73	215.00	0.63	215.50	0.75
265.83	0.57	265.67	0.70	265.50	0.62	266.00	0.71
333.58	0.54	333.42	0.69	333.25	0.61	333.75	0.71
430.25	0.52	430.08	0.67	429.92	0.58	430.42	0.70
503.00	0.49	502.80	0.66	502.70	0.58	503.20	0.68
599.00	0.49	598.80	0.65	598.70	0.57	599.20	0.68
766.33	0.48	766.17	0.62	766.00	0.56	766.50	0.66
1252.58	0.44	1252.42	0.58	1252.25	0.51	1252.75	0.64

March 1998 cells

Cell E1		cell E2		cell E3		cell G1		cell G3		Cell cont2	
Time (hr)	C/Co	Time (hr)	C/Co	Time (hr)	C/Co	Time (hr)	C/Co	Time (hr)	C/Co	Time (hr)	C/Co
1.52	0.95	1.37	1.00	1.27	1.02	1.18	1.06	0.90	1.03	0.83	1.24
19.85	0.91	19.70	0.97	19.60	1.00	19.52	1.00	19.23	0.97	19.17	1.09
68.80	0.84	68.65	0.88	68.55	0.87	68.47	0.89	68.18	0.82	68.12	0.97
163.27	0.71	163.12	0.79	163.02	0.83	162.93	0.82	162.65	0.73	162.58	0.88
235.77	0.62	235.62	0.72	235.52	0.76	235.43	0.74	235.15	0.64	235.08	0.90
331.52	0.60	331.37	0.70	331.27	0.71	331.18	0.74	330.90	0.63	330.83	0.86
402.78	0.51	402.63	0.62	402.53	0.57	402.45	0.60	402.17	0.53	402.10	0.77
499.12	0.54	498.97	0.58	498.87	0.56	498.78	0.57	498.50	0.52	498.43	0.79
668.18	0.50	668.03	0.57	667.93	0.54	667.85	0.58	667.57	0.51	667.50	0.73

Table A2: Continued

April 1998 Cells

Cell ER-1		Cell V2-1		Cell Ga-1		Cell E2-3		Cell E2-2		Cell Ga-2		Cell GI-1		Cell Cont	
time(hr)	C/Co	time(hr)	C/Co	time(hr)	C/Co	time(hr)	C/Co	time(hr)	C/Co	time(hr)	C/Co	time(hr)	C/Co	time(hr)	C/Co
1.08	1.02	1.00	1.00	0.90	0.99	0.85	0.95	0.80	0.99	0.73	1.00	0.65	0.98	0.58	1.03
20.50	0.94	20.42	0.92	20.32	0.86	20.27	0.72	20.22	0.90	20.15	0.94	20.07	0.80	20.00	1.02
50.42	0.87	50.33	0.87	50.23	0.78	50.18	0.62	50.13	0.92	50.07	0.85	49.98	0.84	49.92	0.96
122.00	0.82	121.92	0.85	121.82	0.68	121.77	0.54	121.72	0.74	121.65	0.85	121.57	0.62	121.50	1.01
164.80	0.77	164.72	0.79	164.62	0.64	164.57	0.52	164.52	0.72	164.45	0.78	164.37	0.49	164.30	0.96
213.00	0.76	212.92	0.76	212.82	0.60	212.77	0.48	212.72	0.68	212.65	0.76	212.57	0.46	212.50	0.95
289.28	0.71	289.20	0.72	289.10	0.55	289.05	0.49	289.00	0.67	288.93	0.70	288.85	0.44	288.78	0.91
360.75	0.69	360.67	0.71	360.57	0.52	360.52	0.48	360.47	0.63	360.40	0.69	360.32	0.42	360.25	0.91
455.00	0.65	454.92	0.68	454.82	0.50	454.77	0.48	454.72	0.63	454.65	0.67	454.57	0.42	454.50	0.91
529.00	0.65	524.92	0.68	524.82	0.50	524.77	0.49	524.72	0.61	524.65	0.64	524.57	0.42	524.50	0.89
697.00	0.63	696.92	0.65	696.82	0.48	696.77	0.49	696.72	0.58	696.65	0.61	696.57	0.42	696.50	0.88
861.08	0.61	861.00	0.61	860.90	0.48	860.85	0.47	860.80	0.55	860.73	0.62	860.65	0.41	860.58	0.89
983.08	0.61	983.00	0.58	982.90	0.50	982.85	0.46	982.80	0.55	982.73	0.57	982.65	0.41	982.58	0.88

July 1998 Cells

Cell Jun4v21		Cell Jun4e1		Cell Jun4v1		Cell Jun4e2		Cell Jun5GI1		Cell Jun5R1		Cell Jun5GI2		Cell Jun5spat		Cell cont	
time(hr)	C/Co	time(hr)	C/Co	time(hr)	C/Co	time(hr)	C/Co	time(hr)	C/Co	time(hr)	C/Co	time(hr)	C/Co	time(hr)	C/Co	time(hr)	C/Co
1.08	0.97	1.02	0.97	0.93	0.96	0.88	0.98	0.82	0.95	0.75	0.97	0.67	0.92	0.58	0.89	0.82	1.01
42.33	0.84	42.27	0.85	42.18	0.87	42.13	0.80	42.07	0.84	42.00	0.85	41.92	0.77	41.83	0.89	41.77	1.01
90.45	0.81	90.38	0.76	90.30	0.76	90.25	0.80	90.18	0.71	90.12	0.78	90.03	0.64	89.95	0.79	89.88	0.97
187.00	0.70	186.93	0.68	186.85	0.70	186.80	0.72	186.73	0.65	186.67	0.71	186.58	0.58	186.50	0.74	186.43	0.99
258.58	0.65	258.52	0.61	258.43	0.67	258.38	0.67	258.32	0.61	258.25	0.66	258.17	0.53	258.08	0.70	258.02	0.99
357.83	0.60	357.77	0.56	357.68	0.60	357.63	0.64	357.57	0.53	357.50	0.56	357.42	0.47	357.33	0.60	357.27	0.89
429.08	0.56	429.02	0.55	428.93	0.60	428.88	0.61	428.82	0.63	428.75	0.54	428.67	0.45	428.58	0.57	428.52	0.89
523.08	0.56	523.02	0.54	522.93	0.58	522.88	0.58	522.82	0.48	522.75	0.55	522.67	0.47	522.58	0.69	522.52	0.88
574.58	0.52	574.52	0.50	574.43	0.57	574.38	0.56	574.32	0.48	574.25	0.50	574.17	0.47	574.08	0.54	574.02	0.85
692.83	0.56	692.77	0.52	692.68	0.58	692.63	0.60	692.57	0.52	692.50	0.54	692.42	0.46	692.33	0.56	692.27	0.88
905.00	0.51	904.93	0.49	904.85	0.55	904.80	0.55	904.73	0.47	904.67	0.52	904.58	0.44	904.50	0.51	904.43	0.85
1050.08	0.51	1050.02	0.50	1049.93	0.53	1049.88	0.58	1049.82	0.46	1049.75	0.49	1049.67	0.43	1049.52	0.51	1049.43	0.85
1222.33	0.49	1222.27	0.48	1222.18	0.54	1222.13	0.54	1222.07	0.47	1222.00	0.49	1221.92	0.45	1221.77	0.51	1221.77	0.85

Table A3: Experimental data for reverse radial diffusion experiments: Lissamine

April 1997 Cells

Cell 1		cell 9		cell 10		cell D	
Time (hr)	C/Co	Time (hr)	C/Co	Time (hr)	C/Co	Time (hr)	C/Co
3.27	0.19	3.30	0.15	3.38	0.12	3.43	0.05
23.68	0.18	23.68	0.20	23.65	0.33	23.70	0.05
47.52	0.18	47.52	0.20	50.35	0.33	50.38	0.05
71.25	0.37	71.25	0.35	73.38	0.45	74.42	0.09
95.93	0.61	96.02	0.34	96.07	0.45	96.13	0.09
168.18	0.41	168.23	0.37	168.28	0.57	168.33	0.11
215.62	0.42	215.67	0.38	215.72	0.56	215.77	0.11
242.57	0.49	242.62	0.44	242.67	0.57	242.72	0.11
336.10	0.42	336.15	0.43	336.20	0.61	336.25	0.12
430.45	0.45	430.50	0.46	430.57	0.65	430.62	0.15
526.15	0.49	526.20	0.49	526.25	0.62	526.30	0.15
1031.40	0.49	1031.45	0.49	1031.50	0.62	1031.55	0.15
1200.50	0.37	1200.55	0.40	1200.60	0.53	1200.65	0.18
1536.23	0.36	1536.28	0.33	1536.33	0.46	1536.38	0.17

July 1997 cells

Cell 6		Cell A		Cell B		Cell V1	
Time (hr)	C/Co	Time (hr)	C/Co	Time (hr)	C/Co	Time (hr)	C/Co
0.85	0.04	0.73	0.00	0.65	0.00	0.40	0.04
43.95	0.21	43.83	0.20	43.75	0.20	43.50	0.07
92.05	0.34	91.93	0.30	91.85	0.28	91.60	0.12
163.87		163.77	0.39	163.80	0.35	163.43	0.16
211.92	0.37	211.77	0.41	211.77	0.41	211.35	0.17
332.84	0.43	332.68	0.46	332.68	0.47	332.28	0.23
381.09	0.44	380.93	0.47	380.92	0.48	380.52	0.25
500.70	0.47	500.55	0.52	500.53	0.54	500.13	0.26
572.68	0.53	572.57	0.54	572.55	0.57	572.15	0.30
669.42	0.51	669.30	0.52	669.30	0.51	668.90	0.28

Table A4: Experimental data for reverse radial diffusion experiments: Bromide

April 1997 Cells

Cell 1		cell 9		cell 10		cell D	
Time (hr)	C/Co	Time (hr)	C/Co	Time (hr)	C/Co	Time (hr)	C/Co
3.17	0.04	3.17	0.06	3.17	0.11	3.17	0.00
22.67	0.13	22.67	0.15	22.67	0.35	22.67	0.06
98.22	0.23	98.22	0.26	98.22	0.59	98.22	0.11
169.72	0.33	169.72	0.41	169.72	0.72	169.72	0.16
241.55	0.44	241.55	0.48	241.55	0.58	241.55	0.17
335.13	0.46	335.13	0.51	335.13	0.69	335.13	0.18
430.38	0.49	430.38	0.52	430.38	0.64	430.38	0.28
1031.80	0.52	1031.80	0.51	1031.80	0.66	1031.80	0.34

July 1997 Cells

Cell 6		Cell A		Cell B		Cell V1	
Time (hr)	C/Co	Time (hr)	C/Co	Time (hr)	C/Co	Time (hr)	C/Co
1.33	0.09	1.17	0.06	1.03	0.06	0.90	0.05
44.33	0.18	44.17	0.11	44.03	0.05	43.90	0.08
92.67	0.23	92.50	0.14	92.37	0.13	92.23	0.10
164.25	0.30	164.08	0.17	163.95	0.17	163.82	0.14
212.33	0.32	212.17	0.19	212.03	0.18	211.90	0.16
333.08	0.36	332.92	0.20	332.78	0.15	332.65	0.20
381.33	0.40	381.17	0.19	381.03	0.23	380.90	0.19
500.83	0.44	500.67	0.26	500.53	0.23	500.40	0.20
571.83	0.46	571.67	0.27	571.53	0.26	571.40	0.21
668.50	0.44	668.33	0.27	668.20	0.24	668.07	0.18
764.25	0.39	764.08	0.25	763.95	0.21	763.82	0.17
911.00	0.42	910.83	0.28	910.70	0.28	910.57	0.22
1075.50	0.36	1075.33	0.22	1075.20	0.21	1075.07	0.17

Table A5: Experimental data for forward radial diffusion experiments: Nitrite

July 1997 cells

Cell 6		Cell A		Cell B		Cell V1	
hours	C/Co	time (hr)	C/Co	time (hr)	C/Co	time (hr)	C/Co
1.33	1.12	1.17	1.05	1.03	0.97	0.90	0.95
44.33	0.86	44.17	0.95	44.03	0.92	43.90	0.92
92.67	0.75	92.50	0.89	92.37	0.89	92.23	0.85
164.25	0.68	164.08	0.81	163.95	0.81	163.82	0.82
212.33	0.72	212.17	0.86	212.03	0.85	211.90	0.84
333.08	0.60	332.92	0.78	332.78	0.77	332.65	0.71
381.33	0.58	381.17	0.72	381.03	0.70	380.90	0.68
500.83	0.52	500.67	0.66	500.53	0.65	500.40	0.65
571.83	0.50	571.67	0.67	571.53	0.66	571.40	0.64
668.50	0.50	668.33	0.63	668.20	0.64	668.07	0.62
764.25	0.46	764.08	0.62	763.95	0.61	763.82	0.57
911.00	0.44	910.83	0.56	910.70	0.58	910.57	0.57
1075.50	0.45	1075.33	0.60	1075.20	0.59	1075.07	0.55

Table A6: Experimental data for forward radial diffusion experiments: DFBA

March 1998 cells

Cell 6		Cell E2		Cell E3		Cell G1		Cell G3		Cell con12	
time (hr)	C/Co	time (hr)	C/Co	time (hr)	C/Co	time (hr)	C/Co	time (hr)	C/Co	time (hr)	C/Co
1.67	1.08	1.37	0.80	1.27	0.88	1.18	0.87	0.90	0.89	0.83	0.93
20.00	0.50	19.70	0.72	19.60	0.73	19.52	0.82	19.23	0.89	19.17	0.78
68.95	0.50	68.65	0.67	68.55	0.70	68.47	0.69	68.18	0.76	68.12	0.69
163.42	0.42	163.12	0.62	163.02	0.55	162.93	0.57	162.65	0.53	162.58	0.67
235.62	0.44	235.62	0.58	235.52	0.57	235.43	0.60	235.15	0.55	235.08	0.67
331.67	0.37	331.67	0.53	331.27	0.56	331.18	0.60	330.90	0.56	330.83	0.66
402.93	0.38	402.63	0.55	402.53	0.55	402.45	0.55	402.17	0.53	402.10	0.67
499.26	0.38	499.97	0.56	498.87	0.53	498.78	0.57	498.50	0.52	498.43	0.61

April 1998 cells

Cell ER-1		Cell V2-1		Cell Ga-1		Cell E2-3		Cell E2-2		Cell Ga-2		Cell G1-1		Cell Cont	
time (hr)	C/Co	time (hr)	C/Co	time (hr)	C/Co	time (hr)	C/Co	time (hr)	C/Co	time (hr)	C/Co	time (hr)	C/Co	time (hr)	C/Co
1.08	1.02	1.00	0.99	0.90	0.97	0.85	0.96	0.80	0.98	0.73	0.98	0.65	0.89	0.58	0.96
20.50	0.96	20.42	0.93	20.32	0.92	20.27	0.81	20.22	0.93	20.15	0.97	20.07	0.88	20.00	1.02
50.42	0.91	50.33	0.90	50.23	0.94	50.18	0.71	50.13	0.87	50.07	1.00	49.98	0.76	49.92	0.96
122.00	0.88	121.92	0.90	121.82	0.79	121.77	0.61	121.72	0.79	121.65	0.93	121.57	0.65	121.50	0.98
164.80	0.82	164.72	0.85	164.62	0.72	164.57	0.58	164.52	0.75	164.45	0.84	164.37	0.60	164.30	0.84
213.00	0.81	212.92	0.82	212.82	0.70	212.77	0.51	212.72	0.74	212.65	0.81	212.57	0.55	212.50	0.93
289.28	0.76	289.20	0.80	289.10	0.66	289.05	0.50	289.00	0.72	288.93	0.77	288.85	0.54	288.78	0.91
360.75	0.77	360.67	0.79	360.57	0.63	360.52	0.48	360.47	0.68	360.40	0.77	360.32	0.49	360.25	0.90
455.00	0.71	454.92	0.77	454.82	0.58	454.77	0.47	454.72	0.67	454.65	0.73	454.57	0.49	454.50	0.87
525.00	0.71	524.92	0.74	524.82	0.56	524.77	0.47	524.72	0.68	524.65	0.73	524.57	0.48	524.50	0.85
697.00	0.69	696.92	0.71	696.82	0.53	696.77	0.47	696.72	0.63	696.65	0.70	696.57	0.46	696.50	0.86
861.08	0.65	861.00	0.68	860.90	0.51	860.85	0.46	860.80	0.62	860.73	0.67	860.65	0.44	860.58	0.87
983.08	0.62	983.00	0.63	982.90	0.53	982.85	0.44	982.80	0.56	982.73	0.63	982.65	0.42	982.58	0.84

July 1998 Cells

Cell Jun4v21		Cell Jun4e1		Cell Jun4v1		Cell Jun4e2		Cell Jun5G11		Cell Jun5R1		Cell Jun5G12		Cell Jun5ga1		Cell cont	
time (hr)	C/Co	time (hr)	C/Co	time (hr)	C/Co	time (hr)	C/Co	time (hr)	C/Co	time (hr)	C/Co	time (hr)	C/Co	time (hr)	C/Co	time (hr)	C/Co
1.08	0.98	1.02	0.97	0.93	0.99	0.88	0.98	0.82	0.96	0.75	0.98	0.67	0.94	0.58	1.03	0.52	1.02
42.33	0.85	42.27	0.89	42.18	0.80	42.13	0.92	42.07	0.88	42.00	0.87	41.92	0.84	41.83	0.93	41.77	0.94
90.45	0.83	90.38	0.73	90.30	0.77	90.25	0.81	90.18	0.76	90.12	0.82	90.03	0.70	89.95	0.83	89.88	0.94
187.00	0.76	186.93	0.73	186.85	0.78	186.80	0.77	186.73	0.74	186.67	0.80	186.58	0.66	186.50	0.81	186.43	0.97
258.58	0.72	258.52	0.69	258.43	0.62	258.38	0.72	258.32	0.71	258.25	0.75	258.17	0.60	258.08	0.78	258.02	0.95
357.83	0.66	357.77	0.64	357.68	0.68	357.63	0.70	357.57	0.61	357.50	0.65	357.42	0.53	357.33	0.68	357.27	0.87
429.08	0.63	429.02	0.63	428.93	0.67	428.88	0.67	428.82	0.63	428.75	0.64	428.67	0.49	428.58	0.66	428.52	0.88
523.08	0.62	523.02	0.62	522.93	0.65	522.88	0.64	522.82	0.55	522.75	0.65	522.67	0.51	522.58	0.68	522.52	0.86
574.58	0.59	574.52	0.57	574.43	0.63	574.38	0.62	574.32	0.66	574.25	0.60	574.17	0.51	574.08	0.63	574.02	0.85
692.83	0.63	692.77	0.58	692.68	0.63	692.63	0.64	692.57	0.59	692.50	0.60	692.42	0.47	692.33	0.62	692.27	0.87
905.00	0.59	904.93	0.53	904.85	0.59	904.80	0.57	904.73	0.51	904.67	0.56	904.58	0.45	904.50	0.58	904.43	0.87
1050.08	0.53	1050.02	0.51	1049.93	0.53	1049.88	0.57	1049.82	0.48	1049.75	0.52	1049.67	0.42	1049.58	0.56	1049.52	0.83
1222.33	0.53	1222.27	0.48	1222.18	0.53	1222.13	0.54	1222.07	0.48	1222.00	0.52	1221.92	0.44	1221.83	0.56	1221.77	0.81

MANAGEMENT PERSPECTIVE

Title: The Radial Diffusion Method Applied to Dolostone Core Samples from the Lockport Formation, Smithville, Ontario: Phase II

Author(s): L Zanini, K Novakowski & G Bickerton

NWRI Publication No.: 99- 203

Citation:

EC Priority/Issue:

During the late 1970's and early 1980's a PCB waste management site was operating on the outskirts of the town of Smithville, located approximately 15 km south of Lake Ontario, on the Niagara escarpment. In 1985, it was discovered that PCB oils and associated solvents had penetrated the into the ground and pervaded the upper horizons of the bedrock underlying the site. This resulted in the closure of a local water supply which utilized groundwater from this aquifer. The major problem with trying to cleanup the site is that the contaminants have moved downward into fractures in the bedrock, where it is extremely difficult to predict where and how the contaminants will migrate. A process that may have an impact on contaminant transport is the diffusional movement of the contaminants from the fractures into the adjacent bedrock.

A series of experiments, known as diffusion experiments, were undertaken to evaluate the potential for chemical tracers to move into the rock mass of five different geological units found at the site. The information obtained from these experiments, presented as diffusion coefficients are required to accurately predict the movement of contaminants into the rock mass, the amount of contaminant in the rock, and aid in future studies which assess the transport and fate of contaminants at the Smithville site.

This work supports the EC Business Line: Clean Environment. Improved methods of measuring groundwater velocity in contaminated fractured rock systems will lead to a reduction in the environmental and human health threats posed by toxic substances carried by groundwater in the subsurface.

Current Status:

The report is intended to be released as a NWRI contribution.

Next Steps:

No future work on this project is anticipated at this time.

Environment Canada Library, Burlington



3 9055 1017 7267 0



Environment
Canada

Environnement
Canada

Canada

Canada Centre for Inland Waters

P.O. Box 5050
867 Lakeshore Road
Burlington, Ontario
L7R 4A6 Canada

National Hydrology Research Centre

11 Innovation Boulevard
Saskatoon, Saskatchewan
S7N 3H5 Canada

St. Lawrence Centre

105 McGill Street
Montreal, Quebec
H2Y 2E7 Canada

Place Vincent Massey

351 St. Joseph Boulevard
Gatineau, Quebec
K1A 0H3 Canada

Centre canadien des eaux intérieures

Case postale 5050
867, chemin Lakeshore
Burlington (Ontario)
L7R 4A6 Canada

Centre national de recherche en hydrologie

11, boul. Innovation
Saskatoon (Saskatchewan)
S7N 3H5 Canada

Centre Saint-Laurent

105, rue McGill
Montréal (Québec)
H2Y 2E7 Canada

Place Vincent-Massey

351 boul. St-Joseph
Gatineau (Québec)
K1A 0H3 Canada